# Electronic Supplementary Information

## Hydroxyapatite Nanowire Rich in [Ca–O–P] Sites for Ethanol Direct Coupling Showing High $C_{6-12}$ Alcohols Yield

Qing-Nan Wang,[a] Bai-Chuan Zhou,[a] Xue-Fei Weng,[a] Shao-Pei Lv,[a] Ferdi Schüth,[b] and An-Hui Lu[a,*]

[a] State Key Laboratory of Fine Chemicals, School of Chemical Engineering, Dalian University of Technology, Dalian 116024, P. R. China.

[b] Max-Planck-Institut für Kohlenforschung, Kaiser-Wilhelm-Platz 1, D-45470 Mülheim an der Ruhr, Germany

*Corresponding author： anhuilu@dlut.edu.cn

# Table of Contents

## 1. Experiment section

### Catalyst synthesis

Nanowire-like HAP was synthesized using a modified recipe.[1] Typically, 1.3 g sodium hydroxide, 13.6 mL oleic acid, 15.2 mL ethanol, and 20 mL deionized water were mixed together under mechanical agitation, to which an aqueous solution of $CaCl_2$ (0.22 g in 20 mL deionized water) was then added to form the pale yellow liquid phases. After the ion-exchange process of $Ca^{2+}$ substituting for $Na^+$, a solution of $NaH_2PO_4$ (0.19 g in 10 mL deionized water) was then added dropwise to obtain milk white mixture. This mixture was agitated for about 0.5 h and then transferred to two 50 mL autoclaves, which were sealed and hydrothermally treated at 180 °C for 23 h. After reaction, the recovered precipitate was repeatedly rinsed with ethanol and deionized water (80 °C), and then calcinated at 600 °C for 2 h under static air to obtain hydroxyapatite, denoted HAP-W. Nanofiber-like HAP (HAP-F) was also prepared by this method except doubling the amounts of $CaCl_2$ and $NaH_2PO_4$. No signals of any forms of sodium species were detected over HAP-W and HAP-F via the XPS measurements. Nanorod-like HAP (HAP-R) was synthesized by a conventional method.[2,3] Briefly, an aqueous solution of $Ca(NO_3)_2$ (0.6 M, Sinopharm) was added dropwise to a solution of $(NH_4)_2HPO_4$ (0.4 M, Sinopharm) at room temperature and stirred for 10 min. The system pH was then adjusted to 10.3 with $NH_3 \cdot H_2O$ (25 wt%, Sinopharm). The slurry was stirred for 24 h at 80 °C. After filtration, drying (50 °C in flowing air), and calcination (600 °C for 2 h in static air), white HAP-R was obtained.

### Characterization

Powder X-ray diffraction (XRD) patterns were obtained with a Panalytical X'pert Pro Super X-ray diffractometer using Cu Kα radiation (40 kV, 40 mA, $\lambda$ = 0.15418 nm). Transmission electron microscopy (TEM) images were obtained on JEOL JEM-2100 operated at an accelerating voltage of 200 kV. The actual Ca/P ratio was determined by ICP-OES using an Optima2000DV instrument.

The number and strength of acid/base sites on catalysts surfaces were measured by temperature-programmed desorption (TPD) on a Micromeritics AutoChem II 2920 apparatus. 100 mg catalyst (40-60 mesh) was loaded into a U-shaped quartz tube and pre-treated at 500 °C for 2 h in He, then cooled to 100 °C. At 100 °C, the bed was exposed first to He for 1 h then $CO_2$ or $NH_3$ for 0.5 h, in sequence. Weakly adsorbed $CO_2$ and/or $NH_3$ were removed by sweeping pure He at 100 °C for 2 h. After the sample was cooled to 50 °C, the TPD measurement was conducted in the range 50-600 °C at a heating rate of 10 °C/min in a He flow. Signals for $CO_2$ (m/z = 44) and $NH_3$ (m/z = 15) were monitored using on-line mass spectrometry (MS). For the spent HAP-W, samples were pre-treated at 325 or 500 °C under $N_2$ (or air).

DRIFTS spectra were collected on a Bruker 70V spectrometer equipped with an *in situ* reaction cell (HARRICK) and MCT detector. The catalyst powder (~30 mg) was placed in the cell and pre-treated at 500 °C for 1 h in a flow of $N_2$. Subsequently, the sample was maintained at 300 °C in flowing $N_2$ to collect the background spectrum. Ethanol vapor was fed into the chamber through a bubbler, carried by $N_2$. The amount of ethanol ($5\times10^{-8}$ mol) delivered to the cell was controlled by a sample loop and the saturated vapor pressure at a given temperature. The evolution of surface species was monitored by IR using averaging 128 scans at a resolution of 4 $cm^{-1}$.

## Ethanol coupling activity measurement

For reactivity measurements, the sieved catalyst (40-60 mesh) was loaded into a quartz tube reactor and pre-treated at 500 °C for 2 h in $N_2$ flow prior to reaction. All experiments were carried out under atmospheric pressure with a total gas flow rate of 30 mL/min. Ethanol mixed with CaO (10-20 mesh) to remove slight water, was fed into reactor through a bubbler by $N_2$ carrier. Methane was co-fed with ethanol and used as an inert internal standard to obtain accurate carbon balance. Each data point was obtained after stabilizing about 20 min at 325 °C. The carbon balance was better than 98% at 325 °C in the conversion range of 1-50%. The carbon balance was further confirmed by the TG-MS analysis for the samples after 10 hour operation (Fig. S9). A Gas Chromatograph (GC) with a Flame Ionization Detector (FID), fitted with a FFAP capillary column, was connected to the reactor outlet to analyze the products. Gas products (such as $H_2$) were detected by a thermal conductivity detector (TCD), equipped with molecular sieves 5A and GDX-102 columns, using Ar as carrier. $H_2$ formation rate was quantified by an external standard method. The retention time for each specific component was determined using the corresponding standard chemicals ($C_2$-$C_{12}$ *n*-alcohols). The molecular structure of *n*-/*iso*-products was further confirmed by GC-MS analysis (Agilent 7890A GC interfaced with 5975C MS).

The ethanol conversion and carbonaceous products selectivity were calculated on the basis of moles of carbon in the products, as follows:

$$Conv.\ (\%) = \left(1-\frac{N_{outlet,ethanol}\times A_{outlet,ethanol}\times f_{outlet,ethanol}}{N_{outlet,ethanol}\times A_{outlet,ethanol}\times f_{outlet,ethanol}+\sum_{i\geq 2} N_i\times A_i\times f_i}\right)\times 100\% \quad (1)$$

Product selectivity:

$$Selec.\ (\%) = \frac{N_i\times A_i\times f_i}{\sum_{i\geq 2} N_i\times A_i\times f_i}\times 100\% \quad (2)$$

The carbon number, FID peak area, and response factor of each product are designated $N_i$, $A_i$, and $f_i$, respectively.

## 2. TEM images

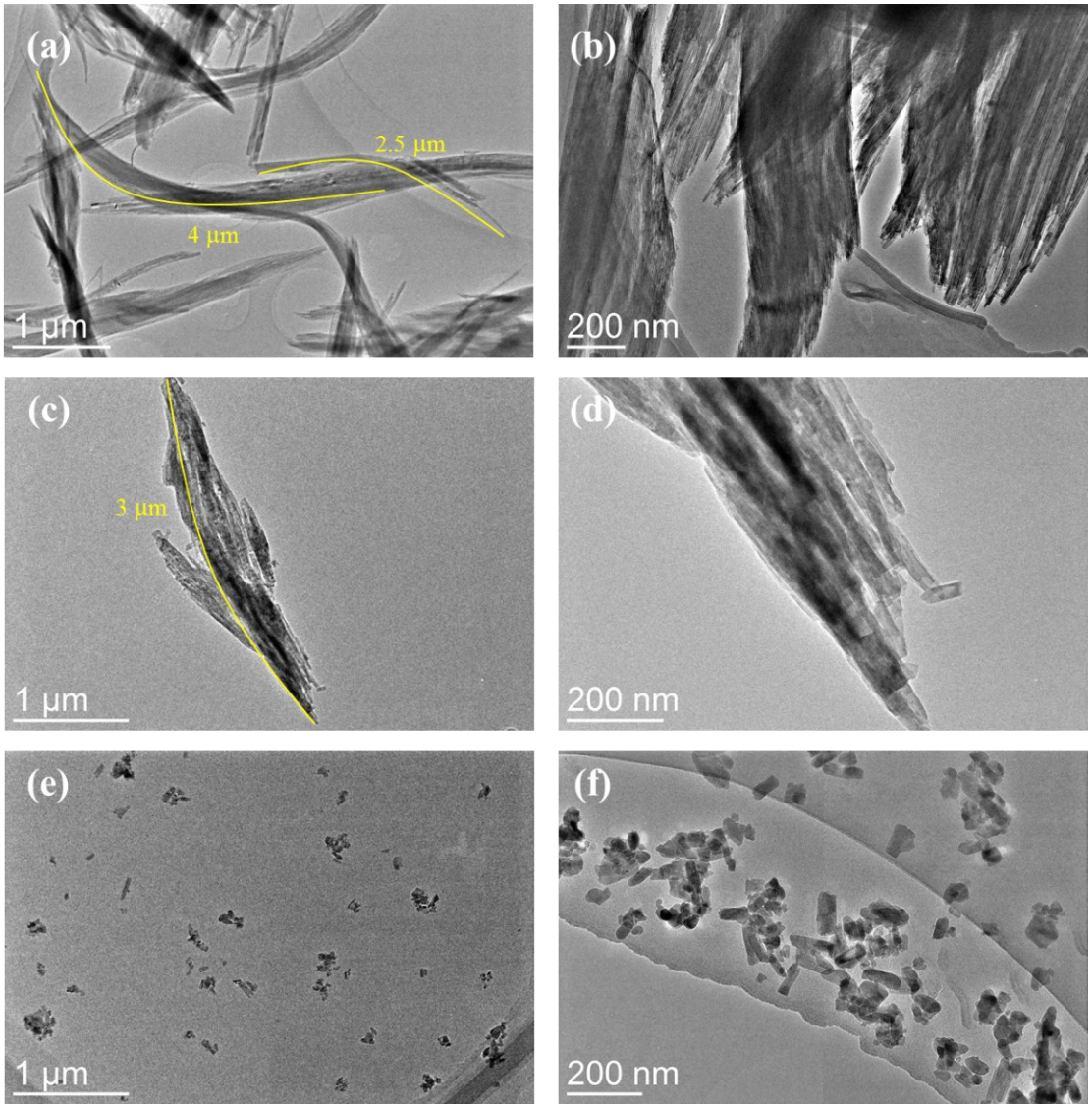


**Fig. S1** TEM images: (a, b) HAP-W, (c, d) HAP-F, and (e, f) HAP-R.

## 3. TEM images

The nanostructure of synthesized HAP samples was detailedly analyzed by HRTEM. Taking HAP nanowire for example (Fig. S2), the shape of this material is almost uniform. The fast Fourier transforms of these HRTEM images (Zone axis: [100]) proved that the preferential growth is exactly along [001] with a- and b-surfaces exposure, i.e., (100) and (010). This result agrees well with the literature reports that HAP tends to grow along the c-axis during wet synthesis on basis of DFT and TEM studies.[4,5]

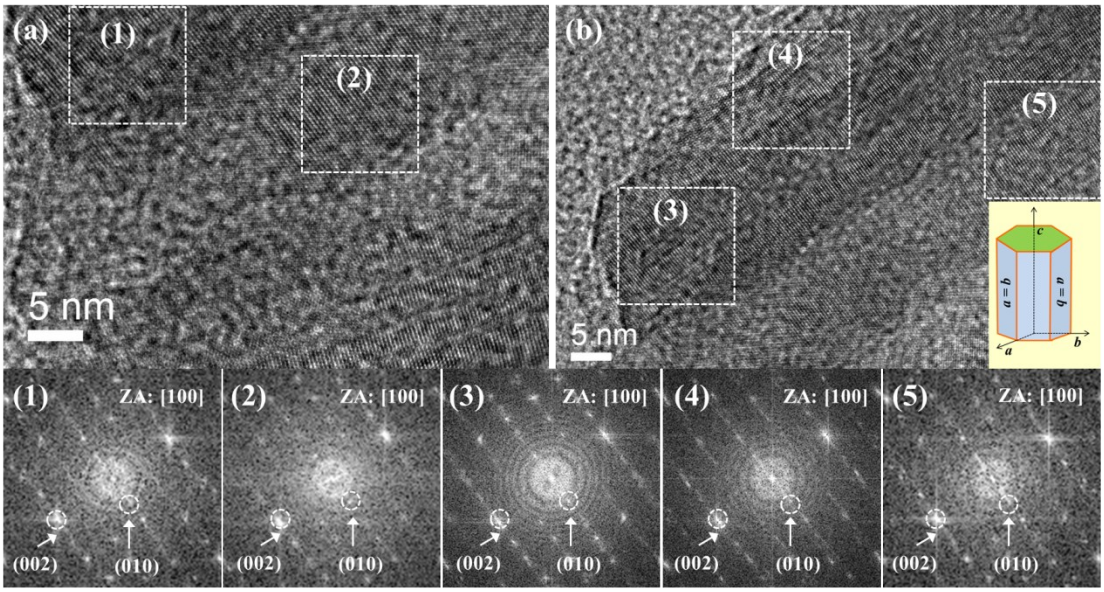


**Fig. S2** HRTEM images of HAP-W.

## 4 List of the main higher aliphatic alcohols

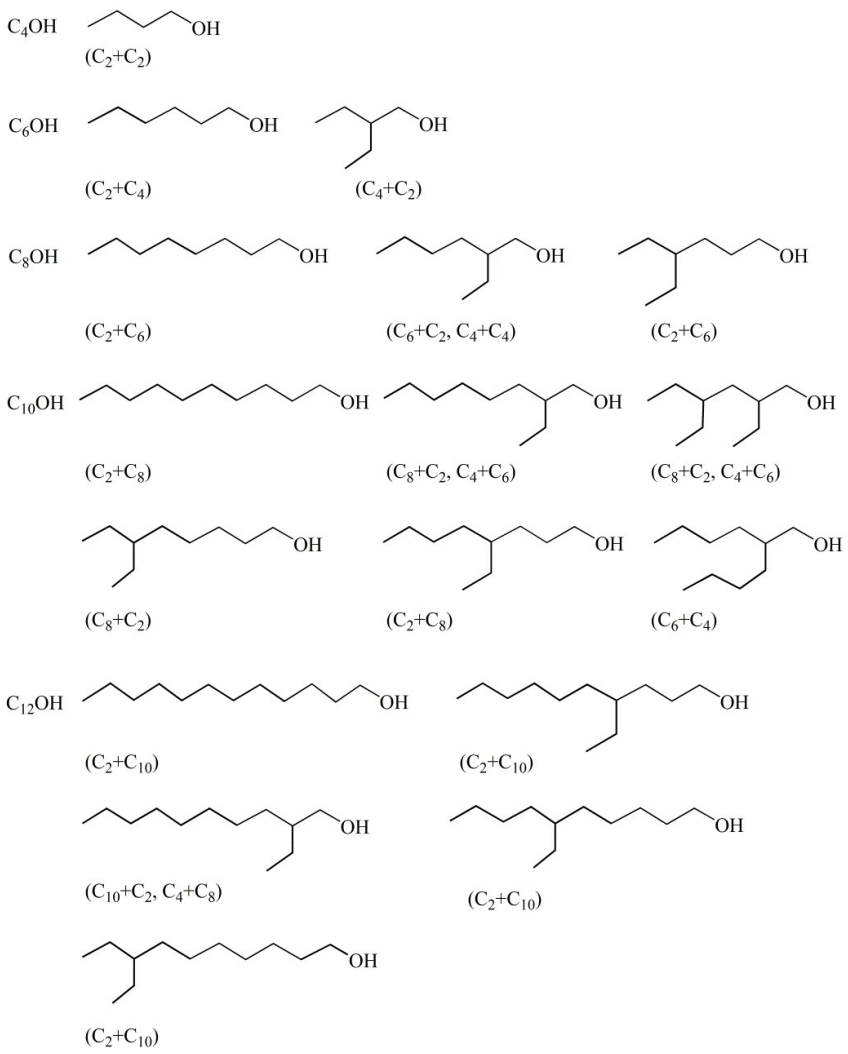


**Fig. S3** List of the observed main higher aliphatic alcohols. Species in parentheses were the reactants which underwent coupling reaction to obtain the specific product, *i.e.*, $C_6OH$ is formed by deprotonation of ethanol ($C_2$) and subsequent C-C bond formation with *n*-butanol ($C_4$).

## 5. Correlation of density of base or acid sites with coupling rate of C-C bonds

We plotted the formation rate of C-C against the density of [Ca–OH], [Ca–O–P], or acid sites, and the ratio of strong base to acid sites. As shown in Fig. S4, a linear relationship indicate that the C-C bond formation is catalyzed by the strong base sites, i.e., [Ca–O–P].

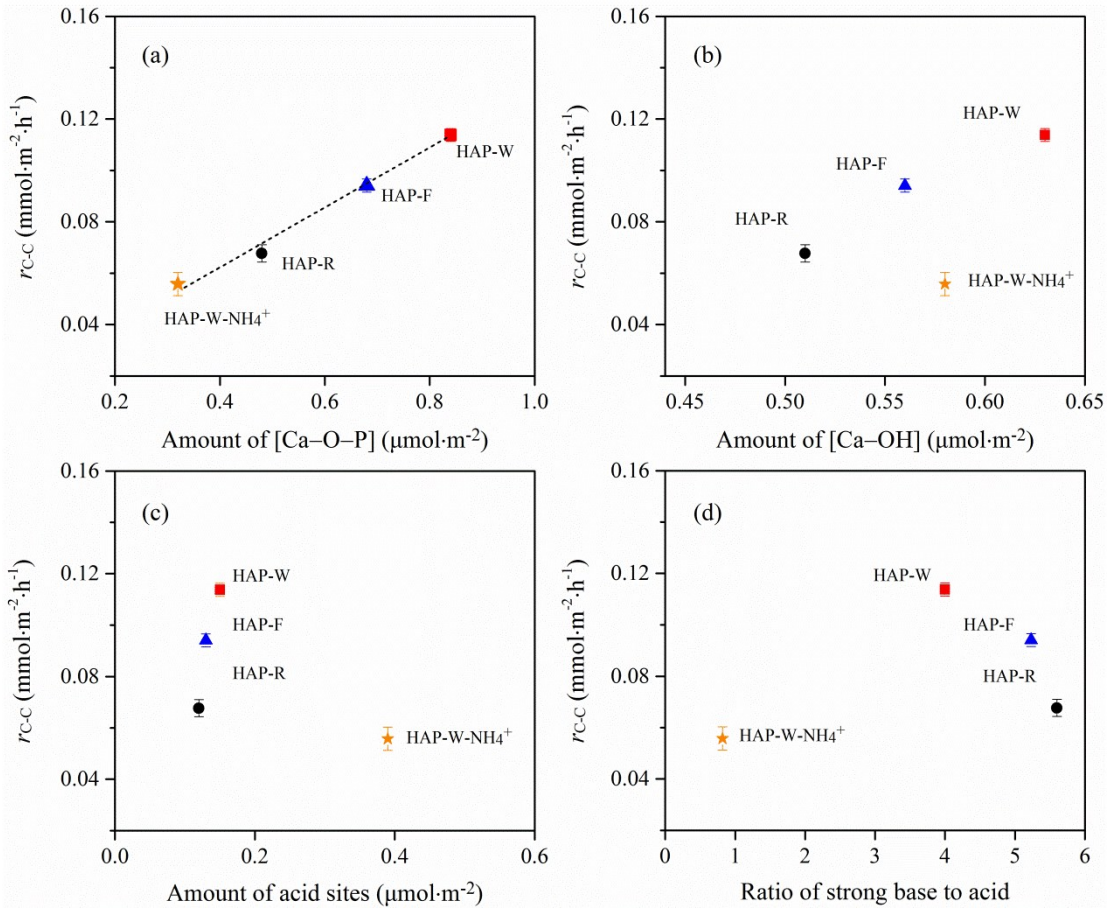


**Fig. S4** Correlation of rate of C-C bond formation with (a) the density of [Ca–O–P] sites, (b) the density of [Ca–OH] sites, (c) the amount of acid sites, and (d) the ratio of strong base to acid. These data were shown in Table S1.

## 6. XRD profile of HAP-W-$NH_4^+$

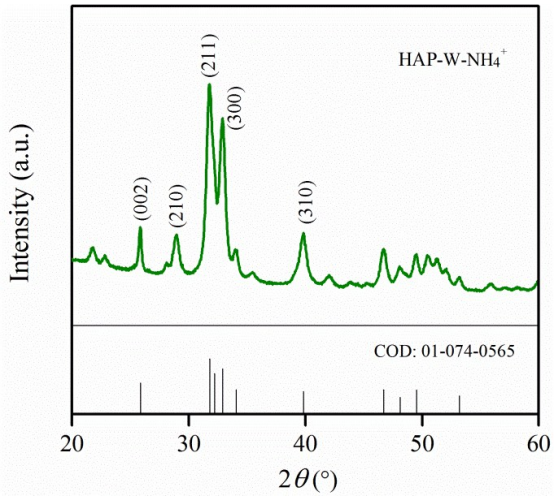


**Fig. S5** XRD profile of HAP-W-$NH_4^+$.

## 7. Surface chemical properties of HAP-W-$NH_4^+$

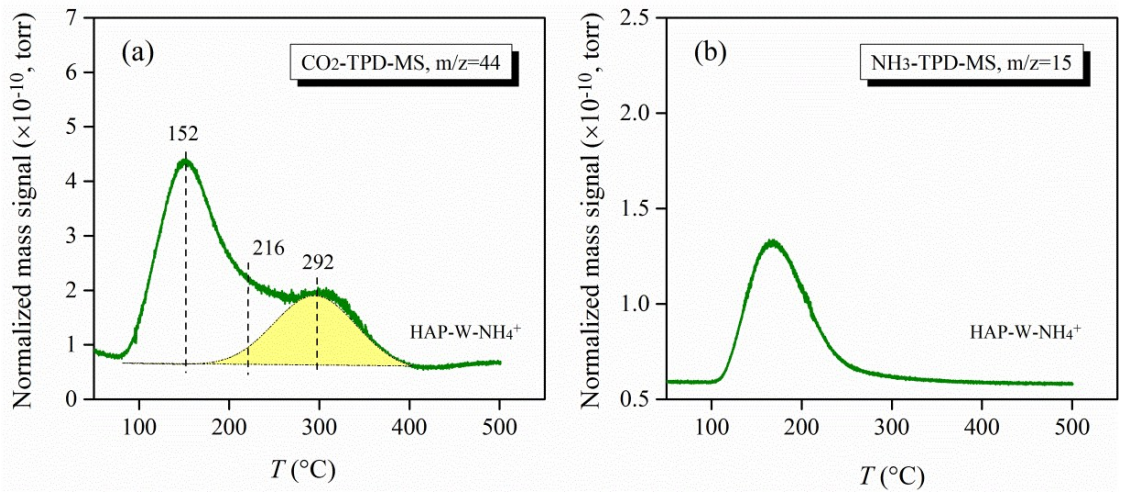


**Fig. S6** (a) $CO_2$- and (b) $NH_3$-TPD-MS profiles of HAP-W-$NH_4^+$.

## 8 Dependence of products selectivity on $H_2$ concentration

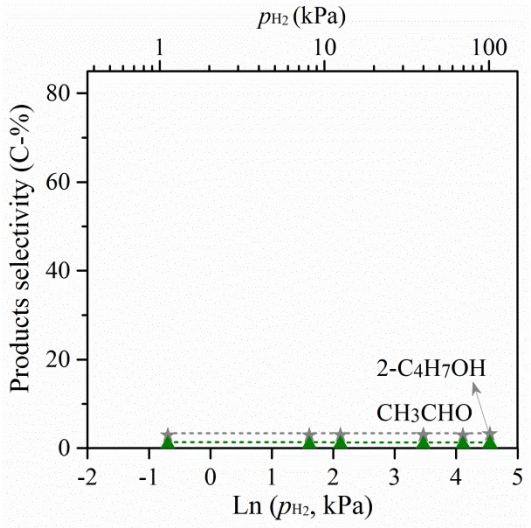


**Fig. S7** Dependence of products selectivity on $H_2$ concentration. Reaction activity was measured over HAP-W at 325 °C in a feed gas of 5.7 vol% $C_2H_5OH$/0.5-94 vol% $H_2/N_2$ with a WHSV of 1.0 $g_{C2H5OH}$ $g_{Cat.}^{-1}$ $h^{-1}$.

## 9 *In situ* IR in ethanol stream flow

*In situ* IR in ethanol stream flow was tested. As seen in the figure below, the signals of C-H (2700-3000 $cm^{-1}$), C=O (1670-1740 $cm^{-1}$, corresponding to aldehydes), O-H (3000-3500 $cm^{-1}$), and C=C (1500-1600 $cm^{-1}$, corresponding to deposited benzene derivatives) were obviously observed after longtime ethanol stream at 30 min. However, although the spent catalyst was treated in only nitrogen or air flow for another 30 min at 300 °C, these IR signals still presented. The signal of the formed acetaldehyde on spent catalysts might be covered by and/or overlapped to that of the carbonaceous deposits, which has aldehyde groups. Therefore, to collect the *in situ* IR spectra right after each dose of ethanol provides a much better method to unravel a clear model of mechanism on fresh HAP. More importantly, our study focused on the reaction route of ethanol on [Ca−O−P] sites of the fresh catalyst, but not on [Ca−OH] and [P−OH] sties of the spent catalyst after longtime on stream.

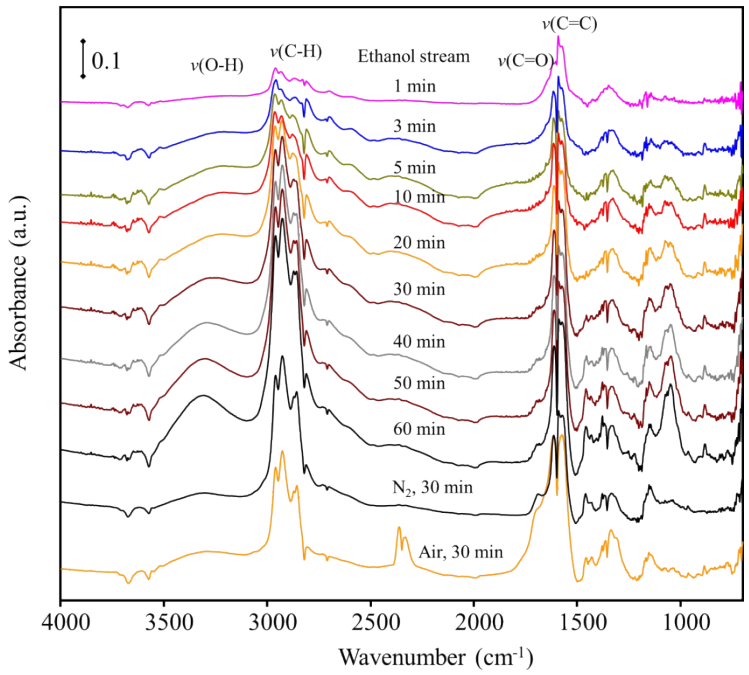


**Fig. S8** *In situ* IR spectra of HAP-W in ethanol stream flow at 300 °C. Reaction activity was measured over HAP-W at 300 °C in stream flow of 5.7 vol% $C_2H_5OH/N_2$.

## 10 TG-MS analysis of the spent catalyst

We checked the carbon buildup on the catalysts by TG under air atmosphere. Fig. S9 shows that ~0.8 wt% of deposited oxygenated carbonaceous species was observed after 10 hours of operation, indicating a >99% carbon balance.

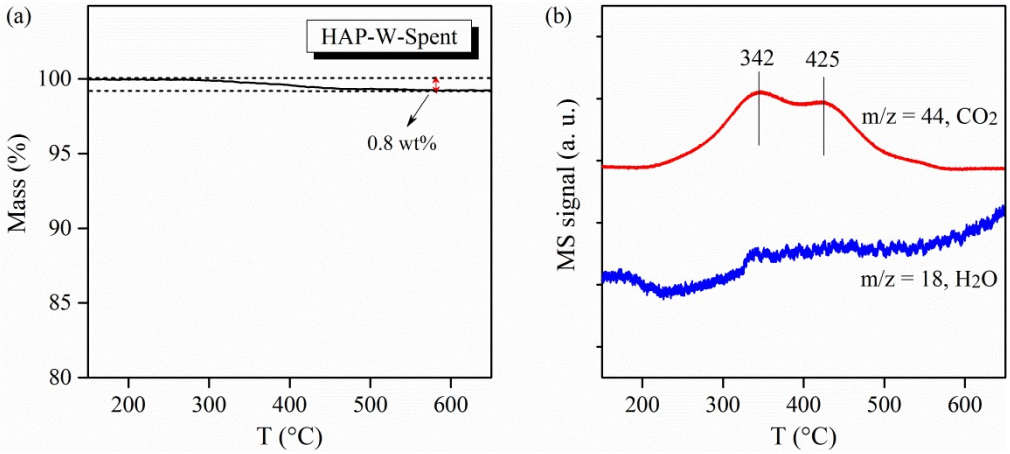


**Fig. S9** TG profiles of HAP-W after 10 h operation at 325 °C, 5.7 vol% $C_2H_5OH/N_2$, and WHSV of 1.0 h.

## 11. Physical and chemical properties of the HAP catalysts

TEM images and $N_2$ adsorption-desorption analysis demonstrate that HAP-R shows obvious mesoporous structure, but HAP-W has only stacked pores. These results are consistent with the different surface area. That is why we normalized the C-C formation rate and the amount of strong basic sites to surface area.

**Table S1.** Physical and chemical properties of the HAP catalysts.

| Catalysts | Ca/P[a] | Surface area ($m^2$ $g^{-1}$)[b] | Aspect ratio[c] | Base amount (μmol $m^{-2}$)[d] | | | Acid amount (μmol $m^{-2}$)[e] |
|---|---|---|---|---|---|---|---|
| | | | | Weak | Medium | Strong | |
| HAP-W | 1.70 | 17 | >400 | 0.63 | 0.04 | 0.84 | 0.15 |
| HAP-F | 1.69 | 20 | 80-200 | 0.56 | 0.06 | 0.68 | 0.13 |
| HAP-R | 1.67 | 32 | 2-5 | 0.51 | 0.06 | 0.48 | 0.12 |
| HAP-W-$NH_4^+$[f] | 1.69 | 20 | - | 0.58 | 0.1 | 0.32 | 0.39 |

[a] Molar ratio determined with ICP. [b] Based on the BET method. [c] From TEM studies. [d] Data measured by $CO_2$-TPD-MS at m/z = 44. [e] Data measured by $NH_3$-TPD-MS at m/z = 15. [f] The suffix "-$NH_4^+$" indicates HAP-W was treated by 0.5 wt% $NH_4NO_3$ aqueous solution at 25 °C for 1 h.

## 12. Catalytic activity of ethanol coupling upon HAP catalysts

**Table S2.** Product distributions of HAP-W, HAP-F, and HAP-R in ethanol coupling reaction.[a]

| Catalysts | Conversion (%)[b] | WHSV ($h^{-1}$) | Reaction rate (mmol $g_{Cat.}^{-1}$ $h^{-1}$) | Formation rate of $H_2$ (mmol $g_{Cat.}^{-1}$ $h^{-1}$) | Selectivity (C-%)[c] | | | | | |
|---|---|---|---|---|---|---|---|---|---|---|
| | | | | | *n*-butanol | $C_6OH$ | $C_8OH$ | $C_{10}OH$ | $C_{12}OH$ | $C_{6\text{-}12}OH$ |
| HAP-W | 5.2 | 5 | 5.65 | 0.38 | 59.5 | 16.2 | 6.9 | 0.9 | 0.2 | 24.2 |
| | 7.9 | 4 | 6.87 | 0.46 | 65.0 | 17.2 | 7.8 | 1.2 | 0.5 | 26.7 |
| | 13.1 | 2.3 | 6.55 | 0.42 | 54.4 | 19.3 | 13.5 | 3.9 | 1.5 | 38.2 |
| | 15.5 | 2 | 6.74 | 0.46 | 54.6 | 20.6 (0.84:1)[d] | 14.7 (1.3:1) | 2.3 | 0.7 | 38.3 |
| | 23.5 | 1.3 | 6.64 | 0.51 | 43.6 | 24.2 | 23.8 | 2.4 | 1.0 | 51.4 |
| | 28.6 | 1.1 | - | - | 46.1 | 24.6 | 20.5 | 2.3 | 0.8 | 48.2 |
| | 30.4 | 1 | 6.59 | 0.45 | 39.9 | 24.1 (0.9:1) | 23.0 (1.1:1) | 5.8 (2.3:1) | 2.0 | 54.9 |
| | 35.7 | 0.91 | - | - | 35.4 | 23.2 | 24.5 | 8.8 | 2.4 | 58.9 |
| | 45.7 | 0.7 | 7.94 | 0.51 | 30.4 | 22.7 (0.91:1) | 25.2 (1.43:1) | 13.1 (2.4:1) | 2.9 | 63.9 |
| HAP-F | 15.2 | 2 | 6.61 | 0.45 | 65.1 | 17.4 (0.86:1) | 8.2 (1.35:1) | 4.5 | 0.2 | 30.1 |
| | 27.7 | 1.1 | 6.62 | 0.49 | 52.1 | 23 (0.87:1) | 15.3 (1.3:1) | 1.5 | 0.5 | 40.3 |
| HAP-R | 6.8 | 4.2 | - | - | 76.0 | 13.2 | 3.7 | 0.7 | 0.1 | 17.9 |
| | 10.2 | 3 | - | - | 71.5 | 15.9 | 6.3 | 0.9 | 0.2 | 23.3 |
| | 15.9 | 2 | 6.87 | 0.45 | 70.1 | 16 (0.88:1) | 7.9 (1.4:1) | 1.0 | 0.2 | 25.1 |
| | 18.4 | 1.7 | - | - | 69.5 | 16.7 | 8.2 | 1.2 | 0.3 | 26.3 |

| | | | | | | | | | |
|---|---|---|---|---|---|---|---|---|---|
| 26.4 | 1.2 | - | - | 62.1 | 18.1 | 10.9 | 1.8 | 0.3 | 32.0 |
| 33.8 | 0.92 | 6.75 | 0.46 | 60.2 | 17.8 (0.8:1) | 11.1 (1.4:1) | 2.2 | 0.3 | 31.1 |
| 40.4 | 0.85 | - | - | 47.9 | 23.9 | 15.6 | 4.7 | 1.5 | 45.7 |
| 46.7 | 0.8 | 6.89 | 0.47 | 50.6 | 20.1 (0.86:1) | 18.1 (1.4:1) | 6.4 (2.3:1) | 1.8 | 46.1 |

[a] Reaction conditions: 325 °C, $C_2H_5OH/N_2$ = 5.7:94.3, $N_2$ 28 mL $min^{-1}$. [b] Ethanol conversion was varied by changing the weight hourly space velocity of ethanol (WHSV). [c] The selectivity of $C_6OH$, $C_8OH$, $C_{10}OH$, and $C_{12}OH$ included a small number of enols. [d] The ratio in parentheses showed the formation rates of branched (*iso*-) to linear (*n*-) products.

## 13. Summary of catalytic activity of ethanol coupling upon different catalysts

**Table S3.** Summary of the catalytic data of some representative catalysts used in ethanol coupling reaction.

| No. | Catalysts | *T* (°C) | WHSV ($h^{-1}$) | Feed composition | Conversion (%) | Reaction rate (mmol $g_{Cat.}^{-1}$ $h^{-1}$) | Selectivity (C-%) | | Ref. |
|---|---|---|---|---|---|---|---|---|---|
| | | | | | | | *n*-butanol | $C_{6-12}$ OH | |
| | HAP-W | 325 | 0.8 | $C_2H_5OH/N_2$ = 5.7:94.3 | 45.7 | 7.9 | 30.4 | 63.9 | **In this work** |
| | HAP-W | 325 | 2.0 | $C_2H_5OH/N_2$ = 5.7:94.3 | 15.5 | 6.7 | 54.6 | 38.3 | |
| | HAP-F | 325 | 2.0 | $C_2H_5OH/N_2$ = 5.7:94.3 | 15.2 | 6.6 | 65.1 | 30.1 | |
| | HAP-R | 325 | 2.0 | $C_2H_5OH/N_2$ = 5.7:94.3 | 15.9 | 6.9 | 70.1 | 25.1 | |
| 1 | Nonstoichiometric HAP | 300 | 1.4 | $C_2H_5OH$/He = 20:80 | 14.7 | 4.5 | 76.3 | 9.8 | [2] |
| 2 | HAP (Ca/P=1.62) | 350 | 1.5 | $C_2H_5OH$/He = 16.4:83.6 | 20 | 6.5 | 39.2 | 3.9 | [3] |
| | HAP (Ca/P=1.65) | 296 | 1.5 | $C_2H_5OH$/He = 16.4:83.6 | 20 | 6.5 | 68.8 | 13 | |
| | HAP (Ca/P=1.67) | 298 | 1.5 | $C_2H_5OH$/He = 16.4:83.6 | 20 | 6.5 | 69.8 | 14.5 | |
| 3 | HAP (Ca/P=1.69) | 350 | 6.2 | $C_2H_5OH$/He = 20:80 | 14 | 18.9 | 50 | 19.4 | [6] |
| | Carbonated HAP (Ca/P=1.69) | 350 | 6.2 | $C_2H_5OH$/He = 20:80 | 14 | 18.9 | 71 | 8.8 | |
| 4 | HAP (Ca/P=1.67) | 325 | 0.7 | $C_2H_5OH$/He = 5.7:94.3 | 17.1 | 2.6 | 63.2 | 24.5 | [7] |
| 5 | HAP (Ca/P=1.62) | 340 | 3.6 | $C_2H_5OH$/He = 5.8:94.2 | 6.6 | 5.2 | 75 | – | [8] |
| | MgO | 380 | 1.08 | $C_2H_5OH$/He = 5.8:94.2 | 7.9 | 1.8 | 40 | – | |
| 6 | Pd/MgO/Graphite | 230 | 1.92 | $C_2H_5OH$/He = 14.3:85.7 | 17 | 7.1 | ~54 | <19 | [9] |
| 7 | 20%Ni/$Al_2O_3$ | 330 | 4.5 | $C_2H_5OH$:100 (12 MPa)[a] | 41.1 | 40.2 | 45.6 | 12.6 | [10] |
| 8 | 4.5%Cu/$Al_2O_3$ | 240 | 4.3 | $C_2H_5OH$:100 (7 MPa) | 14 | 13.1 | 64 | – | [11] |

| | | | | | | | | | |
|---|---|---|---|---|---|---|---|---|---|
| 9 | Mg-Al oxides (Mg/Al=3:1) | 350 | 2.0 | $C_2H_5OH/N_2$=12:88 | 32 | 13.9 | 35 | – | [12] |
| 10 | MgO-$Al_2O_3$ | 300 | 0.05 | - | 45 | 0.5 | 50 | 7 | [13] |
| 11 | 4%NiMgAlO (Mg/Al=4:1) | 250 | 3.2 | $C_2H_5OH/N_2$ = 45:55 (3 MPa) | 18.8 | 13.1 | 55.2 | 31.1 | [14] |
| | | 250 | 3.2 | $C_2H_5OH/N_2$ = 45:55 (3 MPa) | 72 | 50.1 | 11.1 | 2.1 | |
| | | 260 | 3.2 | $C_2H_5OH/N_2$ = 45:55 (3 MPa) | 7 | 4.9 | 42.9 | 2.3 | |
| 12 | 1%CoMgAlO (Mg/Al=3:1) | 400 | 7.9 | $C_2H_5OH$/He = 32:68 | ~38 | 65.3 | ~25 | | [15] |
| 13 | 5%Ir/carbon | 160 | 5 | $C_2H_5OH/H_2O$ = 4:96 | 32(16 h) | 34.8 | ~15 | ~4 | [16] |
| 14 | 3%Cu1%$CeO_2$/Carbon | 250 | - | Ethanol liquid (0.1 MPa) | 31(16 h) | | 41.2 | 20.6 | [17] |
| 15 | 10%Co1%$CeO_2$/Carbon | 250 | 3.2 | $C_2H_5OH/N_2$ = 1:500 (2 MPa) | 34.1 | 23.7 | 47.6 | 18.4 | [18] |
| | 2%Cu1%$CeO_2$/Carbon | | | $C_2H_5OH/N_2$ = 1:500 (2 MPa) | 11.9 | 8.3 | 67.6 | 5.8 | |
| 16 | 2%Pd@UiO-66 | 250 | 3.2 | $C_2H_5OH/N_2$ = 1:250 (2 MPa) | 49.9 | 34.7 | 50.1 | - | [19] |
| 17 | HAP | 275 | - | $C_2H_5OH/H_2$/He = 1:50:50 | 52 | | 55 | 31 | [20] |
| 18 | HAP | 275 | - | $C_2H_5OH/H_2$ = 4.8:95.2 | 3.3 | | 79.2 | 4.5 | [21] |
| | | | | $C_2H_5OH/H_2$ = 4.8:95.2 | 8.2 | | 81.7 | 8.2 | |
| 19 | MgO | 450 | - | - | 56.1 | | 33 | – | [22] |
| | 10%Ba/MgO | | | | 34.2 | | 22.6 | – | |
| | 10%Ca/MgO | | | | 14.6 | | 67.6 | – | |
| 20 | 5%PdMgAlO (Mg/Al=3:1) | 200 | - | Ethanol liquid (0.1 MPa) | 3.8 (5 h)[b] | | 72.7 | – | [23] |
| | 5%CuMgAlO (Mg/Al=3:1) | | | | 4.1 (5 h) | | 40.3 | – | |
| 21 | 10%Cu10%NiMgAlO (Mg/Al=2.4:1) | 310 | - | Ethanol liquid (8 MPa) | 46.7 (6 h) | | 80 | 17.2 | [24] |

[a] Number in parentheses represents that experiments are performed under a specific pressure in a steel autoclave or fixed-bed reactor. [b] Number in parentheses is the reaction time.

## 14. Base properties of the spent HAP-W and the regenerated ones

After longtime ethanol stream, the strong basic [Ca−O−P] sites greatly decreased on the spent HAP-W catalysts even though treated at 325 °C for 2 h under $N_2$ prior to $CO_2$-TPD experiments. When the spent catalyst was treated at 500 °C under air atmosphere, the amount of surface basicity was complete reproducibility compared with the fresh catalysts (Table S1), indicating that the strong basic [Ca−O−P] sites can be completely regenerated after high temperature treatment at air atmosphere. Correspondingly, the catalytic activity was comparable to that of the fresh one.

**Table S4.** Chemical properties of the spent HAP-W catalysts and the ones regenerated at different conditions[a]

| Catalysts | Regeneration atmosphere | T (°C)/t (h)[c] | Base amount (μmol $m^{-2}$)[d] | | | | Reaction rate (mmol $g^{-1}$ $h^{-1}$) |
|---|---|---|---|---|---|---|---|
| | | | Total | Weak | Medium | Strong | |
| HAP-W[b] | Air | 600/2 | 1.51 | 0.63 | 0.04 | 0.84 | 6.7 |
| HAP-W-spent | $N_2$ | 325/2 | 0.31 | 0.21 | 0.05 | 0.05 | 0.9 |
| | Air | 500/2 | 1.42 | 0.59 | 0.04 | 0.79 | 6.5 |

[a] The HAP-W was operation in ethanol stream flow for time-on-stream of 10 h. [b] The data on this fresh sample were from the Table S1. [c] The regenerated temperature and corresponding time. [d] Data measured by $CO_2$-TPD-MS at m/z = 44.

## 15 References


[1] X. Wang, J. Zhuang, Q. Peng, Y. Li, *Adv. Mater.* 2006, **18**, 2031–2034.

[2] T. Tsuchida, S. Sakuma, T. Takeguchi, W. Ueda, *Ind. Eng. Chem. Res.* 2006, **45***,* 8634–8642.

[3] T. Tsuchida, J. Kubo, T. Yoshioka, S. Sakuma, T. Takeguchi, W. Ueda, *J. Catal.* 2008, **259**, 183–189.

[4] C. A. Ospina, J. Terra, A. J. Ramirez, M. Farina, D. E. Ellis, A. M. Rossi, *Colloid. Surface B* 2012, **89**, 15–22.

[5] C. R. Ho, S. Zheng, S. Shylesh, A. T. Bell, *J. Catal.* 2018, **365**, 174–183.

[6] L. Silvester, J.-F. Lamonier, J. Faye; M. Capron, R.-N. Vannier, C. Lamonier, J.-L. Dubois, J.-L. Couturier, C. Calais, F. Dumeignil, *Catal. Sci. Technol.*, 2015, **5**, 2994–3006.

[7] C. R. Ho, S. Shylesh, A. T. Bell, *ACS Catal.* 2016, **6**, 939−948.

[8] S. Hanspal, Z. D. Young, H. Shou, R. J. Davis, *ACS Catal.* 2015, **5**, 1737−1746.

[9] C. López-Olmos, M. V. Morales, A. Guerrero-Ruiz, C. Ramirez-Barria, E. AsedegbegaNieto, I. Rodríguez-Ramos. *ChemSusChem* 2018, **11**, 3502–3511.

[10] P. Dziugan, K. G. Jastrzabek, M. Binczarski, S. Karski, I. A. Witonska, B. Kolesinska, Z. J. Kaminski, *Fuel* 2015, **158**, 81–90.

[11] T. Riittonen, K. Eranen, M. -A. Päivi, A. Shchukarev, A.-R. Rautio, K. Kordas, N. Kumar, T. Salmi, J.-P. Mikkola, *Renew Energy* 2015, **74**, 369–378.

[12] D. L. Carvalho, R. R. de Avillez, M. T. Rodrigues, L. E. P. Borges, L. G. Appel, *App. Catal. A* 2012, **415–416**, 96–100.

[13] K. K. Ramasamy, M. Gray, H. Job, D. Santosa, X. S. Li, A. Devaraj, A. Karkamkar, Y. Wang, *Top. Catal.* 2016, **59**, 46–54.

[14] J. Pang, M. Zheng, L. He, L. Li, X. Pan, A. Wang, X. Wang, T. Zhang, *J. Catal.* 2016, **344**, 184–193.

[15] J. Quesada, L. Faba, E. Díaz, S. Ordóñez, *App. Catal. A* 2018, **559**, 167–174.

[16] Q. Liu, G. Xu, X. Wang, X. Mu, *Green Chem.*, 2016, **18**, 2811–2818.

[17] D. Jiang, X. Wu, J. Mao, J. Ni, X. Li, *Chem. Commun.* 2016, **52**, 13749−13752.

[18] X. Wu, G. Fang, Z. Liang, W. Leng, K. Xu, D. Jiang, J. Ni, X. Li, *Catal. Commun*. 2017, **100**, 15–18.

[19] D. Jiang, et al. *ACS Catal.*, 2018, DOI: 10.1021/acscatal.8b04014.

[20] T. Moteki, A. T. Rowley, D. W. Flaherty, *ACS Catal.* 2016, **6**, 7278−7282.

[21] T. Moteki, D. W. Flaherty, *ACS Catal.* 2016, **6**, 4170−4183.

[22] A. S. Ndou, N. Plint, N. J. Coville, *App. Catal. A* 2003, **251**, 337–345.

[23] I.-C. Marcu, N. Tanchoux, F. Fajula, D. Tichit, *Catal. Lett.* 2013, **143**, 23–30.

[24] Z. Sun, A. C. Vasconcelos, G. Bottari, M. C. A. Stuart, G. Bonura, C. Cannilla, F. Frusteri, K. Barta, *ACS Sustainable Chem. Eng.* 2017, **5**, 1738−1746.